

RSC Advances



This is an *Accepted Manuscript*, which has been through the Royal Society of Chemistry peer review process and has been accepted for publication.

Accepted Manuscripts are published online shortly after acceptance, before technical editing, formatting and proof reading. Using this free service, authors can make their results available to the community, in citable form, before we publish the edited article. This *Accepted Manuscript* will be replaced by the edited, formatted and paginated article as soon as this is available.

You can find more information about *Accepted Manuscripts* in the [Information for Authors](#).

Please note that technical editing may introduce minor changes to the text and/or graphics, which may alter content. The journal's standard [Terms & Conditions](#) and the [Ethical guidelines](#) still apply. In no event shall the Royal Society of Chemistry be held responsible for any errors or omissions in this *Accepted Manuscript* or any consequences arising from the use of any information it contains.

Zinc Induced Polyelectrolyte Coacervate Bioadhesive and its Transition to Self-healing Hydrogel

Weina Wang^{1,2,//} Yisheng Xu,^{1,//*} Ang Li¹, Tao Li¹, Miaomiao Liu¹, Regine von Klitzing²,
Christopher K. Ober³, A. Basak Kayitmazer⁴, Li Li¹ and Xuhong Guo^{1,5*}

¹State Key Laboratory of Chemical Engineering, East China University of Science and
Technology, Shanghai 200237, China.

²Stranski-Laboratorium für Physikalische und Theoretische Chemie, Technische Universität
Berlin, Strasse des 17. Juni 124, D-10623 Berlin, Germany

³Department of Materials Science and Engineering, Cornell University, Ithaca, NY 14853-
1501, USA

⁴Chemistry Department, Bogazici University, Bebek, Istanbul 34342, Turkey

⁵Key Laboratory of Materials-Oriented Chemical Engineering of Xinjiang Uygur Autonomous
Region and Engineering Research Center of Materials-Oriented Chemical Engineering of
Xinjiang Bingtuan, Shihezi University, Xinjiang 832000, China

//These two authors contributed equally to this work.

*To whom correspondence should be addressed. E-mail: yshxu@ecust.edu.cn (Yisheng Xu)
and guoxuhong@ecust.edu.cn (Xuhong Guo)

Abstract: To mimic the underwater adhesion of marine mussels, bioadhesive has been prepared with poly(acrylic acid) backbone functionalized with 30% catechol appendants. The polyelectrolyte chains can be reversibly crosslinked through metal chelation and irreversibly gelled by oxidative crosslinking. Surprisingly, the reported “poor” metal chelator Zn^{2+} not only imparts this injectable adhesive with much superior adhesion after the formation of coacervation compared to the one chelated by stronger metal crosslinker (eg. Fe^{3+}), but also generates good mechanical performance of self-healing hydrogel after the oxidation of catechol groups with a pH trigger. Such pH-responsive material with strong adhesion and good self-healing property at different conditions could be an ideal candidate in biomedical adhesion and tissue engineering.

Keywords: Polyelectrolyte; bioadhesive; self-healing; hydrogel; coacervation.

1. Introduction

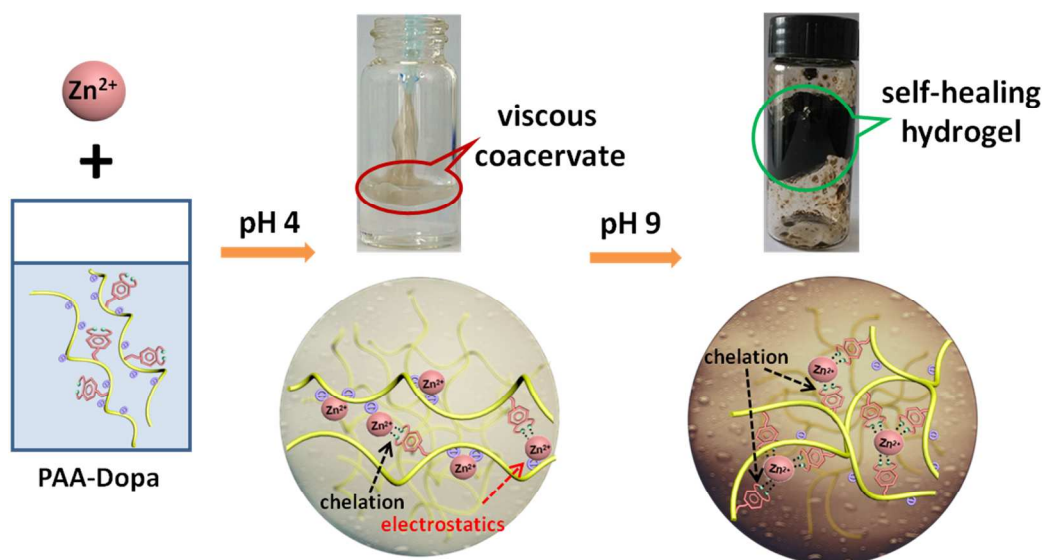
The development of novel biomaterials plays an essential role in the successful use of wound sealants in surgery. However ideal wound sealant has been a challenging topic for decades because tissue engineering process requires biocompatible material with excellent wettability to get injected and spread on wound precisely. In addition effective curing and adequate mechanical properties are indispensable to maintain stability in situ. Dopa-modified polymeric structures inspired by marine organisms such as mussels and sandcastle worms living in a harsh seawater environment have garnered increasing interest to explore biomimetic

adhesives for tissue engineering or other medical purposes particularly for use in wet environment. The key functional groups are catechol side chains which can be easily crosslinked by metal ions¹ to form catechol complexes (mono-, bi-, and tris- complex). On the other hand, such structures can also undergo chemical/enzymatic oxidation²⁻⁴ to form stable covalent bonds with bidentate H-groups⁵ and thus possess enough cohesive force for good performance adhesives.

A number of recent investigations have focused on the improvement of adhesive properties of bioadhesives using metal chelated hydrogels probably because of the difficulty of using strong oxidants in biological systems. The metal chelated catechol system were proposed to be ideal candidates for tissue adhesive and sealant.^{6,7} Some alternative backbones have been used such as poly(ethylene glycol) (PEG),^{7,8} polystyrene⁹ or hyaluronic acid (HA)¹⁰ to enhance adhesive performance. These polymers demonstrate performance competitive to commercial super glues after crosslinking even though they exhibit very dark color of the materials after curing. Nevertheless, the fact that metal ions harden the material gives self-healing ability on the bulk scale which somehow limits the adhesive performance of the materials (several hundred kPa level).⁶ As noticed,^{6,11} the oxidation process reduces adhesive force and provides enough cohesive force for adhesives, while metal chelation strongly enlarges the cohesive force range, hence facilitating the formation of hydrogels.

In this work, an novel water-based polymeric adhesive with good bonding strength and fast in situ sealing capabilities is presented as effective tissue adhesive and orthopedic sealant.¹² Interestingly, this material is based on a delicate Dopa functionalized poly(acrylic acid) in the presence of weak divalent cross-linker Zn^{2+} . Zn^{2+} was rarely used in Dopa containing polymers since it showed little crosslinking in most polymeric backbone system.¹³

In current study, poly(carboxylic acid) such as poly(acrylic acid) (PAA) was chosen as the backbone because of its high sorption capacity to chelate metal ions¹⁴ and the highly soluble electrolytic property which can take place of the protein polyamide chain of mussel adhesive protein. Since mussels concentrate Zn^{2+} more than 100,000-fold higher in the adhesive plaque compared to its concentration in sea water.¹⁵ In addition, zinc supplementation has been found to improve wound healing in zinc-deficient cases,¹⁶ Zn^{2+} was hence chosen to be the metal chelator. In the absence of catechol groups, complex formation of Zn^{2+} with PAA by electrostatics in an aqueous acidic environment (low pH) shows no adhesion but a turbid solution.¹⁷ By partially conjugating catechol groups to PAA backbone, the anionic characteristics of the polymers are retained. Taking advantage of “sticky” features of the catechol group, the adhesive force can be maximized when a coacervate is created from PAA-Dopa in the presence of Zn^{2+} at low pH (Scheme 1).



Scheme 1. Biomimetic adhesive and hydrogel induced by pH in the presence of Zn^{2+} .

The interactions between PAA-Dopa and Zn^{2+} can be manipulated by external conditions to sequentially form high performance coacervate adhesive (strong adhesion, electrostatic interactions) to hydrogel (good stress recovery, coordinate and covalent interactions) in a simple process. The optimization of the cohesive and adhesive forces imparts the material with both hardness and adhesive properties.¹¹ In principle, such complex coacervate adhesive can instantly form after being injected at low pH and then gelled at elevated pH. This system is probably ideal for tissue repair even though many practical issues still need to be carefully considered from the aspect of medical purposes.

2. Experimental

2.1 Materials

Poly(acrylic acid) (PAA) ($M_w = 250$ kg/mol, 35 wt% in H_2O), Dopamine hydrochloride, 1-methyl-2-pyrrolidinone (NMP) (99.5%), N,N'-dicyclohexylcarbodiimide (DCC), N-Hydroxysuccinimide (NHS) (98%), sodium tetraborate ($Na_2B_4O_7$), sodium bicarbonate ($NaHCO_3$), ethyl acetate ($C_4H_8O_2$), zinc chloride ($ZnCl_2$) were purchased from Sigma Aldrich. PAA solution was freeze dried and ground to white powder before experiments. Other chemicals were used without further purification.

2.2 Synthesis and purification of PAA-Dopa

The synthesis was based on our previous report.¹⁸ Because of the highly reactive property of dopamine moiety, dopamine hydrochloride was initially stored under moderately basic conditions in an aqueous solution of sodium borate and sodium bicarbonate, where the medium protected dopamine moiety from side reactions by forming borate ester.¹⁹ After grafting, the pH of aqueous solution was reduced to less than pH 2 in order to deprotect the dopamine moiety. PAA-Dopa was then extracted with ethyl acetate.²⁰ This synthesis was carried out under nitrogen. The product of PAA-Dopa powder is water-soluble. In a typical run, PAA (1.0 g, 13.9 mmol -COOH groups) was dissolved in NMP (20 ml) at 60 °C for 24 h. DCC (0.587 g, 2.845 mmol) and NHS (0.058 g, 0.5 mmol) were introduced into the PAA solution under magnetic stirring for 2 h for the following use. Na₂B₄O₇ (1.144 g, 5.69 mmol) and NaHCO₃ (0.478 g, 5.69 mmol) were dissolved in NMP (30 ml) under vigorous stirring and bubbled with N₂ for 0.5 h. Dopamine hydrochloride (1.841 g, 9.71 mmol) was then added for another 0.5 h mixing, followed by dropwise addition of well-prepared PAA mixture. The reaction mixture was stirred overnight at room temperature with N₂ bubbling. Finally, the pH of reaction solution was reduced to less than 2 and precipitated three times with ethyl acetate (250 ml in total). For further purification, the crude wet product was dissolved into DI water (30 ml) and dialyzed (SpectraPor 3 tubing, molecular weight cutoff: 14000 g/mol) against DI water in dark until the conductivity of water outside the bag reached constant. The final product was freeze dried to get PAA-Dopa powder which was then stored in a sealed container.

2.3 Preparation of Zn²⁺ crosslinked coacervate/hydrogel

PAA-Dopa with a catechol percentage of ~30 mol% was dissolved in pH 4 acetate buffer (0.35 M of Dopa). Zn^{2+} solution with different concentration was introduced into PAA-Dopa solution with the same volume. Coacervate was instantly formed. At pH ~9 this material was triggered the formation of self-healing hydrogel. For better comparison of hydrogel with different crosslinking degrees, these pH triggered hydrogels were then allowed to settle for 1~3 hours in an air tight container to facilitate complete diffusion and relaxation of the polymer network.

2.4 UV-vis Spectroscopy with PAA-catechol and Zn^{2+}

Dopamine grafting stoichiometry was determined in pH 4 acetate buffer with an SHIMADZU 2550 spectrophotometer using a 1 cm path length quartz cuvette. The catechol group displays a characteristic peak at λ_{279} nm ($\lambda_{279} = 2600 \text{ M}^{-1}\text{cm}^{-1}$).²¹ Same volume of PAADopa (0.35 M, pH 4 buffer) and Zn^{2+} (with stoichiometric $\text{Zn}^{2+}/\text{Dopa}$ of 1.4, 3.2, 4.0, and 8.0, respectively) were mixed and magnetically stirred for 2 h and centrifuged, after which certain amount of the supernatant was diluted with deionized water to keep λ_{max} inside the linear absorption range ($\lambda_{\text{max}} < 1$).

2.5 Rheology

All rheological measurements were performed by MCR501 rheometer from Anton-Paar Physical (Austria) equipped with the 25 mm parallel plate geometry. In brief, same volume of Zn^{2+} and PAA-Dopa (0.35 M, pH 4) solutions were added onto the rheometer baseplate.

Water-born adhesives formed after gentle stirring for a few seconds. Soft adhesives were extruded on the platform. To study the transition temperature of water-born adhesives with different cross-linking degree (Zn^{2+} concentration of 0.5, 0.7, and 1.4 M), measurements were performed at a frequency of 1 Hz and a strain of 1% and the temperature was ramped from 25 to 45 °C at a rate of 0.5 °C/min. To investigate the stable self-healing property, strain was increased from 0.1 to 1000 % in 200 s to break the structure of hydrogel after which the recovery process was monitored by small amplitude oscillation at 1% strain for another 200 s. The strain-recovery tests were repeated five times. To compare the dynamic rheological properties between coacervates and hydrogels, and by extension, the nature of the metal-ligand crosslinks, frequency sweeps were performed under different crosslinking degree in the linear viscoelastic range at constant strain amplitude of 1% from 1 to 100 rad/s at room temperature.

2.6 Lap shear adhesion testing

Lap-shear adhesion tests were conducted with a Hengyi HY-0580 tensile test instrument with a 3000 N loading cell. The loading rate was 5 mm/min to reach an ultimate force for all samples. Different adherends (1 cm × 2 cm) of aluminum, stainless steel, polyethylene (PE) and Teflon were used for these tests. Adherends were first polished with aluminum oxide cloth (120#) followed by washing with hexanes, ethanol, acetone, deionized water and finally air-dried overnight. Additional washes and scratches have to be employed to get rid of insoluble residues if necessary. Zinc chloride solution (200 uL, 1.4 M) was evenly spread over one adherend, followed by PAA-Dopa solution (200 μL, 0.35 M of catechol group) on top of it. Two adherends were overlapped to fulfill an area of 1 cm × 2 cm, pressed together squeezing

out a small excess of adhesive and clamped. For each sample, 5 trials were conducted. For dry curing method, samples were first pressed for 1 h at room temperature (20 °C). Then they were cured at 40 °C for 22 h and finally cooled at room temperature (20 °C) for 1 h.²² For semi-wet curing method, samples prepared above were subsequently stored underwater at room temperature for another day. For wet curing method, fresh bonded specimens with water-born adhesives were immediately incubated underwater at room temperature for 24 h. The shear strength was immediately measured after the samples were taken out of water. A widely used commercial α -cyanoacrylic resin adhesive was used by simple mixing A, B glues together (2:1 by weight, 15 mg in total) for comparison.

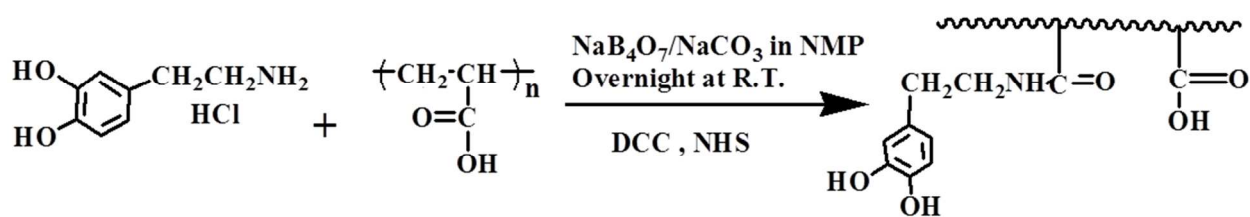
2.7 Other characterizations

The morphology of coacervate droplets was examined with a LEIKA DM 2500P PLM. Images were captured with a charge-coupled device camera connected to a PC via a WT-1000GM imaging board. FT-IR spectra were obtained with a Nicolet 6700 instrument (Nicolet Instrument, Thermo Company, USA) over the wave number range of 4000-1000 cm^{-1} . ^1H -NMR spectra were recorded on a BRUKER AVANCE 500 spectrometer operating at 500 MHz with D_2O as solvent. SEM results of surface morphology of lyophilized adhesives and hydrogels were obtained by NOVA Nano SEM 450 with an accelerating voltage of 3 keV. Before analysis, a thin Au film was coated for conductivity.

3. Results and discussion

3.1 Synthesis of catechol modified polymer

Synthesis of PAA-Dopa was illustrated in Scheme 2. The PAA used here has an average molecular weight of 250 kDa. The appearance of a stretching peak at 1645 cm^{-1} and bending peak at 1544 cm^{-1} by transmission infrared spectroscopy (Figure S1, supporting information) indicates the successful attachment of dopamine groups. Approximately 30% of carboxylate groups were grafted with dopamine through an amidation reaction demonstrated by NMR (Figure S2, supporting information). Furthermore, the adjustment of the adhesive and cohesive force by pH can induce a transition of adhesive to hydrogel in a simple dopa-metal system in the presence of Zn^{2+} . The resulted adhesive demonstrates strong adhesion in both dry and aqueous states with no need of strong oxidants compared to the same type of underwater adhesives currently reported.^{10,21-23}



Scheme 2. Synthesis scheme of PAA-Dopa.

From UV-vis spectra, the characteristic peak of the hydroxyl moiety at 279 nm^{21} was used to estimate the grafting degree of catechol groups on the PAA backbone as shown in Figure S3a, supporting information. As noticed, Dopa groups grafted on the PAA chains remain in

their reduced states without being oxidized: no shoulder between 310 and 380 nm was observed implying no formation of α , β -dehydro Dopa intermediates.²⁴ This means good protection of the reactions from oxygen. The grafting density ranges from 15% to 40% as the Dopa/AA ratio increases from 0.2 to 1 (Figure S3a and b, supporting information). In this work, 30% of grafting density was chosen because this ratio is consistent to the catechol content in foot protein 5 from the common blue mussel (*M. edulis*)²⁵ which contains the highest Dopa content among all marine adhesive proteins.

3.2 Zinc induced electrostatically driven coacervation

At fixed Dopa grafting ratio (30%), PAA-Dopa solution was injected into zinc solution at different concentrations. Dense coacervate was immediately formed (video, supporting information). As the zinc concentration was increased, the free catechol groups on PAA chains in the supernatant decreased reflecting the increase of catechol chelation degree (Figure S3c and d, supporting information). However, the free catechol concentration did not change as the Zn^{2+} : Dopa ratio is greater than 4. The resulted adhesives exclusively manifest high viscosity and grey color. The results here are somehow different from previous results found in Fe^{3+} systems in which mono-catechol- Fe^{3+} complexes dominate and no crosslinking exists at low pH conditions.^{26,27} Since Zn^{2+} has a lower charge density than iron as a consequence of its larger size and lower charge, weaker complexation with catechol groups is expected to form mono-catechol- Zn^{2+} complexes. Meanwhile, zeta potentials of PAA and PAA-Dopa are -16.8 and -22.6 mV respectively (Figure S4) at pH 4 where quite a few carboxylic groups are dissociated and negatively charged, hence it is more likely to have electrostatic interactions

during the formation of coacervate. It is believed that the electrostatic interaction between positively charged Zn^{2+} (chelated with catechol groups) and negatively charged carboxylic groups from another polymer chain can certainly facilitate the formation of inter-polymeric complexes (Scheme 1) and hence certain cohesive force was reached.

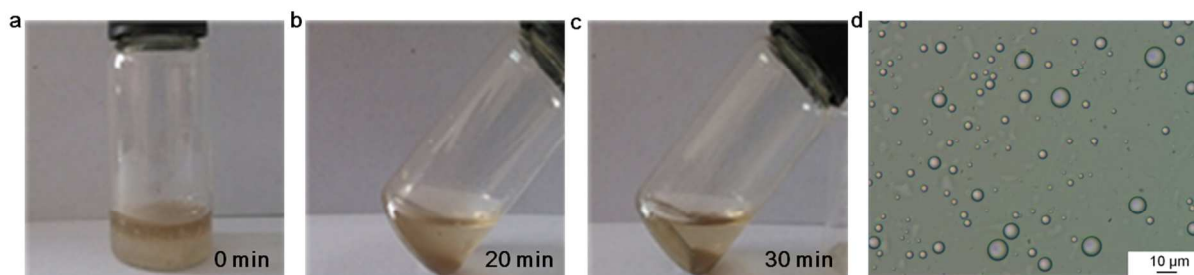


Figure 1. Fluidity of the coacervate (Zn^{2+} : Dopa = 1.4:1, pH = 4). (a, b and c) When injecting PAA-Dopa liquid into Zn^{2+} solution, adhesives form and condense at the bottom after 20-30 minutes. (b) Microscopic view of coacervate droplets.

The formation of complex adhesive and the condensation from aqueous solution can be identified from Figure 1 through visual and microscopic observations. The rapid progress of such complexation leads to further neutralization of the complex and finally to the formation of coacervate in the presence of Zn^{2+} . This also explains the previous findings that Zn^{2+} often promotes hardness properties when mixed with polycarboxylate polymers.¹³ As a comparison, addition of Zn^{2+} to simple PAA or Dopa solution does not form viscous liquid phase or provides any adhesion. Without the negatively charged structure and the sticky sidechain, the material does not generate enough cohesive or adhesive force to function as an adhesive.

A lower elastic modulus (G') than viscous modulus (G'') determined by rheology analysis (Figure 2a) indicates fluidic properties at low pH (~ 4) especially at low Zn: Dopa ratios. The curves of G' and G'' as a function of frequency crossed each other, and the cross points shifts to lower frequency as the Zn: Dopa ratio was raised. This means that the relaxation time τ^* ($\tau^* = 1/f^*$) becomes longer, where f^* is the crossover frequency at $G' = G''$. The τ^* suggests the time scale of the mechanical relaxation in the polymeric structure. A larger τ^* reflects a stronger attractive interactions between polymer chains²⁸ as expected since more cationic Zn added facilitates both chelation and columbic interactions.

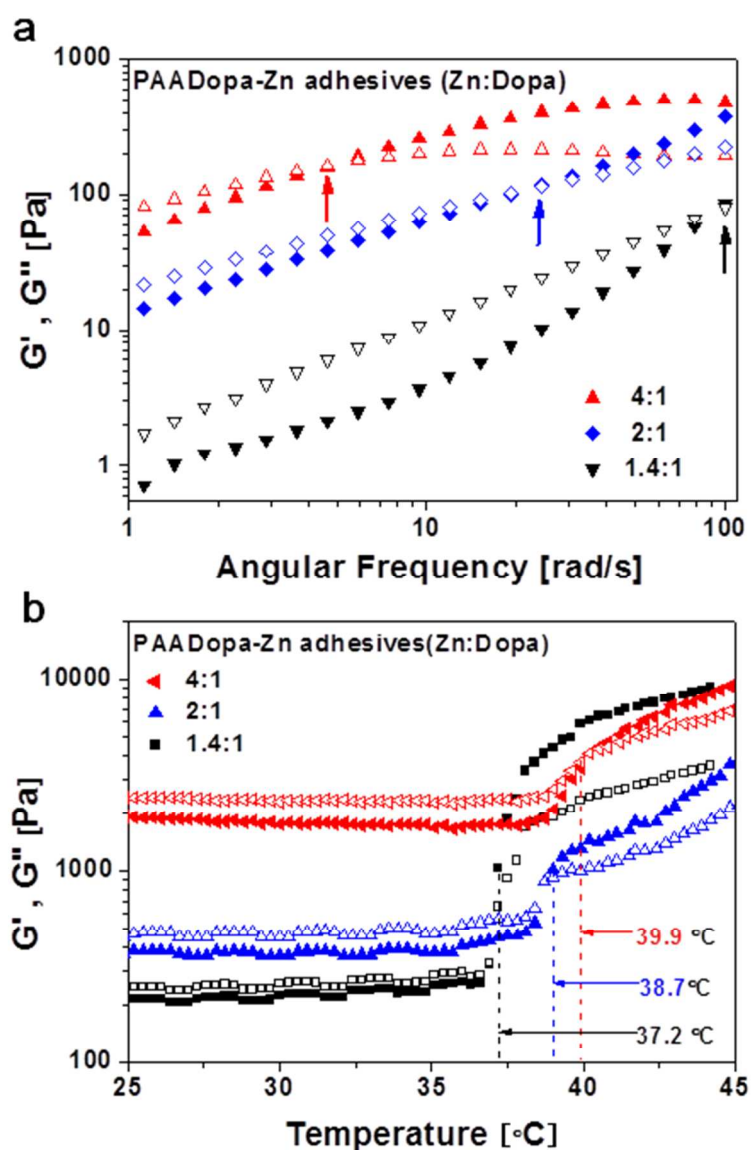


Figure 2. Rheometry of zinc cross-linked PAA-Dopa adhesives at pH 4. (a) With different Zn: Dopa ratios at a strain of 1% and at room temperature (arrow shows the crossover point) (b) The solidification or gelation temperature test at frequency of 1 Hz. In both figures, storage G' and loss G'' modulus are represented by closed and open symbols, respectively).

In Figure 2b, the temperature dependence of G' and G'' was investigated to reveal the phase transition behaviors of such adhesive. Three kinds of samples with different zinc ratios were studied and the cross points of G' and G'' can be clearly observed as the samples transform from liquid-like to gel-like samples. The overall response to temperature is between 37 and 40 °C likely suggesting a superior intrinsic feature for physiological temperature response. An enhancement of sample stoichiometry (Zn: Dopa) does not increase the transition temperature dramatically. Under conditions of the test set-up, the possible oxidative crosslinking is excluded by the remained light color of the adhesives. Therefore the transition temperatures are mainly due to the physical phase change of the adhesive.²¹

The quantitative lap shear mechanical analysis (as shown in Figure S5) of adhesive strength in both dry and wet states was performed on different types of substrates including aluminum, stainless steel, polyethylene (PE) and Teflon. The results are presented in Figure 3a and b. In general, adhesives on rough metal surfaces with high free energy perform much better and this is similar to the cases of mussel adhesion on different substrates.^{22,29} In the curing process, a temperature (40 °C) near physiological temperature was chosen as the curing temperature and samples were cured for at least 24 hours to ensure the complete solidification on all substrates. After curing, Dopa groups in all samples were automatically aerobic oxidized

either in air or in water suggested by the dark color observed at the end. Therefore it is concluded that the crosslinking between Dopa groups took place revealing the mechanism for solidification.

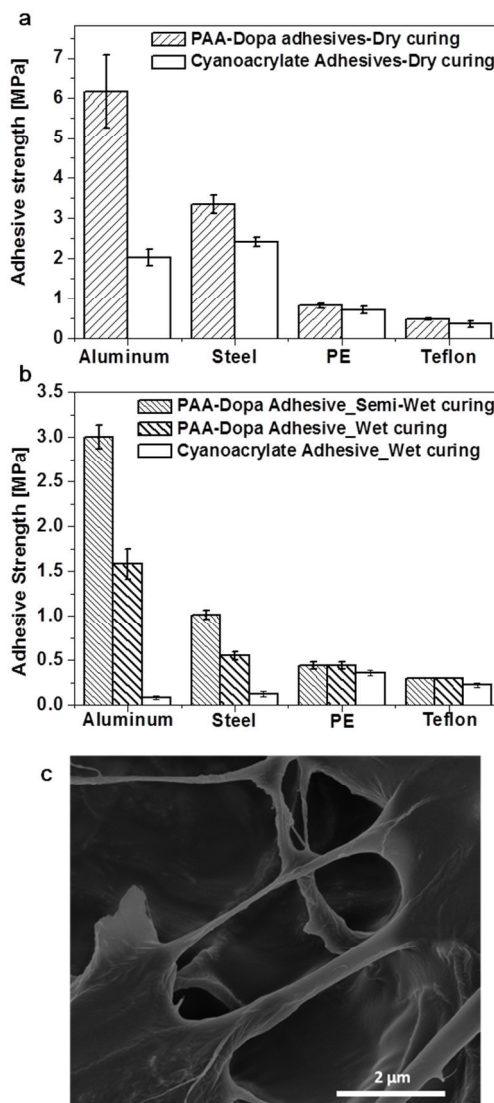


Figure 3. Comparison between PAADopa adhesives and commercial glue in force-versus-extension of adhesion test on different substrates with (a) dry curing and (b) wet/semi-wet curing method. (c) SEM Image of lyophilized adhesives (Scale bar represents 2 μm) which

indicates the adhesive stretching feature. “Semi-wet curing” means that curing was performed in air for one day followed by another day immersion in water and the bonded strength was tested immediately as the sample was removed from water; “Wet curing” means that curing was performed in water for one day and bond strength was measured immediately as the sample was removed from water.

For all cases, the coacervate adhesives perform better than popular commercial glue (α -cyanoacrylic resin adhesive) especially on aluminum substrates. Compared to other cases for the dry adhesion, the adhesion of coacervate (as shown in Table 1) was around 9-fold of the commonly Fe^{3+} incorporated adhesive¹³ and around 20-fold of mussel adhesive.²⁹ Surprisingly, it is even much higher than white glue.²² In the case of wet adhesion, adhesives were cured underwater for 24 hours and then immediately measured after removing from water. The wet adhesion strength is about more than four times of the natural P. California adhesive.^{21,30,31}

Table 1. Lap Shear Adhesive Strength (MPa) Data Compared with other adhesives of good dry adhesion on aluminum substrates

Mussel ^a	Dopa modified ^b polymer- Fe^{3+}	White glue ^c	α -Cyanoacrylic ^d resin adhesive	PAADopa - Zn^{2+} ^e
0.28	0.71	4.01	2.20	6.17

Curing conditions: ^aAt ambient temperature for 18h,²⁹ ^{b,c}At 55 °C for 24h,¹³ ^{d,e}At 40°C for 24 h.²²

The performance is also much better than other metal-chelated Dopa based adhesives (as shown in Table 2).^{21,32} SEM result shown in Figure 3c indicates the stretching of PAADopa-Zn²⁺ coacervate after curing. Apparently, the material possesses certain cohesion forming the network and also exhibits adhesive property as expected.

Table 2. Lap Shear Adhesive Strength Data Compared with other high performance adhesives by wet curing method

P. California^a	Dopa modified polymer-Fe³⁺^b	Polyphospho-dopamide-Mg²⁺^c	α-cyanoacrylic resin adhesive^d	PAADopa-Zn²⁺^e
0.35	0.15	0.65	0.08	1.58

Curing conditions: ^athe estimated bond strength of the natural P. California adhesive on glass;²¹

^bCured underwater for 24 h on aluminum substrates;³² ^cCured on aluminum substrates underwater for 24 h at 37 °C;³³ ^{d,e}Cured on aluminum substrates for 24 h at room temperature.

3.3 pH induced transformation from adhesive to hydrogels

Interestingly, a further increase of pH to 9 favors the formation of a hydrogel. These results are consistent with the iron mediated Dopa system reported previously.^{6,26,34} When pH was greatly increased, Dopa groups were oxidized accompanied by the appearance of dark color. The ionization of hydroxyl group enhances the chelating capability to Zn and therefore enables the crosslinking between zinc and two Dopa moieties.⁵ The only difference is that the weak coordination effects of zinc-Dopa system need a higher pH for gelation even though the

zinc amount added is much greater than that of iron system because of the weaker chelation force of zinc. On the other hand, the electrostatic interaction between Zn and PAA can't be excluded at higher pH condition, but the simple addition of PAA into zinc solution does not generate a gel structure (just turbid solution) suggesting the gelation is mainly induced by the coordination between zinc and Dopa groups. Compared to the coacervate adhesives studied above, the elastic modulus (G') of the hydrogel, as presented in Figure 4, is larger than the viscous modulus (G'') displaying a gel structure. The higher mechanical property of the gel structure is obtained by the irreversible oxidation of catechol group at higher pH which means the adjusting to less adhesive and more cohesive structure.

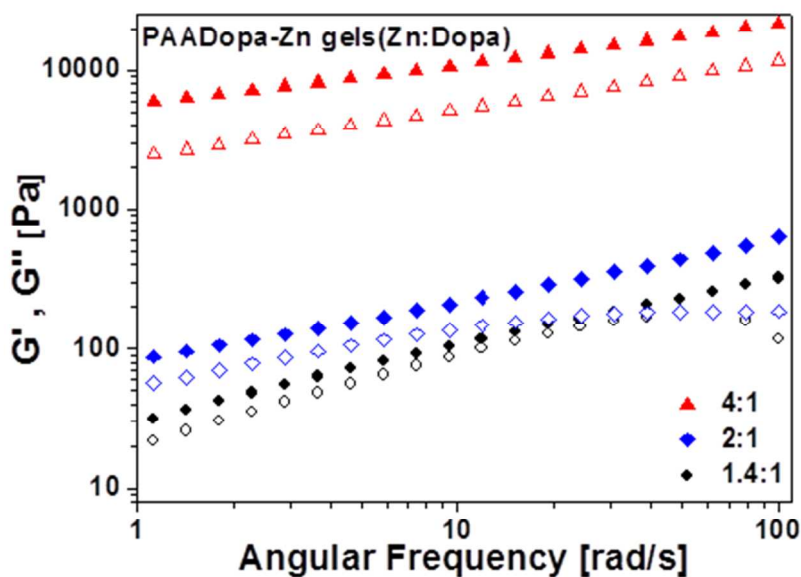


Figure 4. Hydrogel formed after pH jump to pH 9. Frequency sweep at different Zn : Dopa ratios (storage G' and loss G'' modulus, closed and open symbols, respectively).

The gel also exhibits excellent self-healing properties. With rheometry straining the hydrogel until failure and afterward monitoring the recovery by small amplitude oscillation, the elastic moduli shown in Figure 5a reveals the excellent restoration performance regardless of zinc content. The hydrogel with highest crosslinking degree recovered in less than 200s to a high storage modulus (G') of 12600 Pa which is close to the initial value of 13100 Pa therefore confirming that the reversible coordinate crosslinking nature of the complex catechol- Zn^{2+} bonds imparts this robust material with self-healing properties. Such quick recovery performance shows comparable or even better performance to Fe-gels.^{26,27}

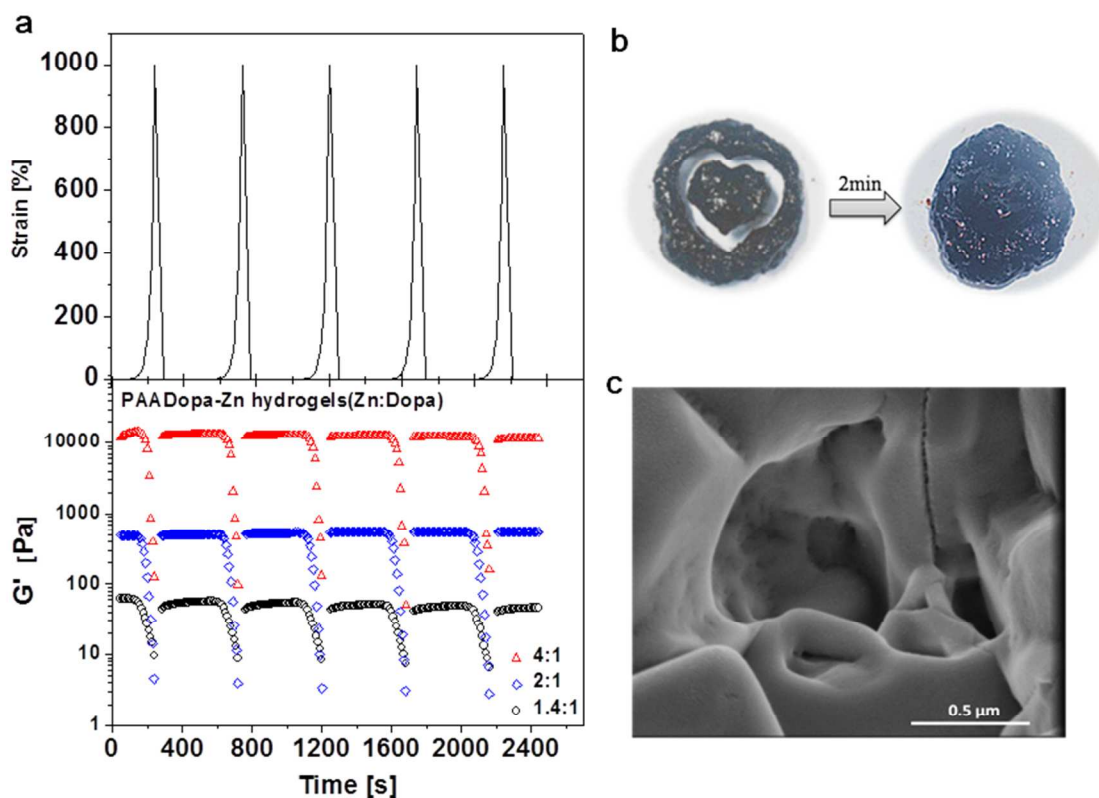


Figure 5. Hydrogel formed after pH jump to pH 9. (a) Recovery tests of hydrogels with different Zn: Dopa ratios in quantitative by shearing hydrogels with increasing strain from 0.1

to 1000% in 200 s to break the structure after which the recovery process was monitored by small amplitude oscillation at 1% strain for another 200 s; (b) In the qualitative tests, a hydrogel at pH 9 was forced to fracture with a heart-shape mode and allowed to recover; (c) SEM image of lyophilized hydrogel (Scale bar represents 0.5 μm).

The self-healing ability was displayed in visual test by cleaving the hydrogel with a heart-shape mode (Figure 5b). After the recovery of the external structure in two minutes, pulling and lifting the gel confirmed the recovered mechanical strength. SEM image from Figure 5c also indicates the porous structure in contrast to the adhesive structure mentioned in Figure 3c. Furthermore, the incorporated Zn^{2+} ions can be removed by aqueous solution containing agent such as ethylene diamine tetraacetic acid (EDTA) as mentioned in Fe^{3+} chelating system²⁶ which indicates the metal-chelating plays a significant role in the present system (Figure S6, supporting information).

4. Conclusions

A pH triggered zinc mediated coacervate was achieved based on Dopa-grafted PAA. It shows extraordinary adhesive performance under both dry and wet conditions. The maximum bonding strength on aluminum in the wet state can reach 1.5 M Pa. This study is superior to previous reports in terms of adhesion strength in both dry and wet states since metal ions simply crosslink polymers forming self-healing hydrogels. The mechanism of the formation of the extra coacervate state is proposed to involve the zinc chelated mono-catechol group

electrostatically interacting with negative charged carboxylic groups from PAA chains and leading to a quick generation of the dense fluidic coacervates. In addition, the coacervate undergoes gelation by increasing pH, hence providing an ideal material for tissue adhesion with simultaneous therapeutical drug delivery at the adhesion point.

Supporting Information

FT-IR and $^1\text{H-NMR}$ spectra of PAA-Dopa. UV-vis detection of Dopa content. Zeta potential of PAA and PAA-Dopa at different pHs. Preparation of lap-shear test and the example of original data. EDTA treatment of zinc cross-linked PAA-Dopa hydrogel.

Video of the coacervation process is available free of charge via the internet at <http://pubs.rsc.org>.

Acknowledgments

Yisheng Xu and Xuhong Guo acknowledge the financial support from the National Natural Science Foundation of China (No. 51273063, 21476143, and 21306049), the Fundamental Research Funds for the Central Universities, the higher school specialized research fund for the doctoral program (222201313005 and 222201314029), 111 Project Grant (B08021), the Open Project of State Key Laboratory of Chemical Engineering (SKL-ChE-14C01) and Firmenich. Weina Wang acknowledges the China Scholarship Council.

References

1. J. H. Waite, N. H. Andersen, S. Jewhurst, C. Sun, *J. Adhesion* 2005, **81**, 297-317.
2. M. Yu, J. Hwang, T. J. Deming, *J. Am. Chem. Soc.* 1999, **121**, 5825-5826.
3. C. Fant, K. Sott, H. Elwing, F. Hook, *Biofouling* 2000, **16**, 119-132.
4. P. A. Suci, G. G. Geesey, *J. Colloid Interface Sci.* 2000, **230**, 340-348.
5. B. K. Ahn, D. W. Lee, J. N. Israelachvili, J. H. Waite, *Nat. Mater.* 2014, **13**, 867-872.
6. B. J. Kim, D. X. Oh, S. Kim, J. H. Seo, D. S. Hwang, A. Masic, D. K. Han, H. J. Cha, *Biomacromolecules* 2014, **15**, 1579-1585.
7. D. G. Barrett, D. E. Fullenkamp, L. He, N. Holten-Andersen, K. Y. C. Lee, P. B. Messersmith, *Adv. Funct. Mater.* 2013, **23**, 1111-1119.
8. D. G. Barrett, G. G. Bushnell, P. B. Messersmith, *Adv. Healthcare Mater.* 2013, **2**, 745-755.
9. H. J. Meredith, C. L. Jenkins, J. J. Wilker, *Adv. Funct. Mater.* 2014, **24**, 3259-3267.
10. H. Lee, Y. Lee, A. R. Statz, J. Rho, T. G. Park, P. B. Messersmith, *Adv. Mater.* 2008, **20**, 1619-1623.
11. J. J. Wilker, *Nat. Chem. Biol.* 2011, **7**, 579-580.
12. H. T. Peng, P. N. Shek, *Expert Rev. Med. Devic.* 2010, **7**, 639-659.
13. G. Westwood, T. N. Horton, J. J. Wilker, *Macromolecules* 2007, **40**, 3960-3964.
14. M. Palencia, B. L. Rivas, E. Pereira, A. Hernández, P. Prádanos, *J. Membrane Sci.* 2009, **336**, 128-139.
15. T.L. Coombs, P.J. Keller, *Aquatic Toxicology*. 1981, **1**, 291-300.
16. E.A. Wilkinson, and C.I. Hawke, *Cochrane Database Syst. Rev.*, CD001273, 2000.
17. D. J. Ennigrou, M. Ben Sik. Ali, M. Dhahbi, *Desalination* 2014, **343**, 82-87.

18. X. Guo, A. A. Abdala, B. L. May, S. F. Lincoln, S. A. Khan, R. K. Prud'Homme, *Polymer* 2006, **47**, 2976-2983.
19. P. Glass, H. Chung, N. R. Washburn, M. Sitti, *Langmuir* 2009, **25**, 6607-6612.
20. H. Lee, B. P. Lee, P. B. Messersmith, *Nature* 2007, **448**, 338-341.
21. H. Shao, R. J. Stewart, *Adv Mater* 2010, **22**, 729-733.
22. C. R. Matos-Pérez, J. D. White, J. J. Wilker, *J. Am. Chem. Soc.* 2012, **134**, 9498-9505.
23. J. D. White, J. J. Wilker, *Macromolecules* 2011, **44**, 5085-5088.
24. B. P. Lee, J. L. Dalsin, P. B. Messersmith, *Biomacromolecules* 2002, **3**, 1038-1047.
25. N. Bandara, H. Zeng, J. Wu, *J Adhes Sci Technol* 2012, **27**, 2139-2162.
26. M. Krogsgaard, M. A. Behrens, J. S. Pedersen, H. Birkedal, *Biomacromolecules* 2013, **14**, 297-301.
27. N. Holten-Andersen, M. J. Harrington, H. Birkedal, B. P. Lee, P. B. Messersmith, K. Y. C. Lee, J. H. P. Waite, *Natl. Acad. Sci.* 2011, **108**, 2651-2655.
28. X. Guo, F. Deng, L. Li, R. K. Prud Homme, *Biomacromolecules* 2008, **9**, 1637-1642.
29. J. R. Burkett, J. L. Wojtas, J. L. Cloud, J. J. J. Wilker, *J. Adhesion*, 2009, **85**, 601-615.
30. H. Shao, K. N. Bachus, R. J. Stewart, *Macromol. Biosci.* 2009, **9**, 464-471.
31. R. J. Stewart, C. S. Wang, H. Shao, *Adv. Colloid Interface Sci.* 2011, **167**, 85-93.
32. J. Nishida, M. Kobayashi and A. Takahara, *J. Polymer Sci. Pol. Chem.*, 2013, **51**, 1058-1065.
33. C. Sun, G. E. Fantner, J. Adams, P. K. Hansma, J. H. Waite, *J. Exp. Biol.* 2007, **210**, 1481-1488.
34. M. S. Menyo, C. J. Hawker, J. H. Waite, *Soft Matter* 2013, **9**, 10314-10323.